**International Journal of Information Technology (IJIT)**
Volume 5, Issue 1, January-June 2024, pp. 1-23, Article ID: IJIT_05_01_001
Available online at https://iaeme.com/Home/issue/IJIT?Volume=5&Issue=1
ISSN Online: 2251-2809, Journal ID: 4573-3410
Impact Factor (2024): 12.52 (Based on Google Scholar Citation)



# CONSTRUCTION OF COMPORTMENTS QUANTITIES UNDULATION THROUGHOUT HUB RARER MORTISE CRUSHING ON SECURE MANACLES

**Dr. Saravanan Suba Ph.D**
Associate Professor, Department of Computer Science,
Government Arts and Science College, Srivilliputtur - 626 125, Tamilnadu, India

**Dr. Dinesh Senduraja Ph.D**
Research Associate (RA), MED & COS, Defence Research & Development Organisation,
(DRDO) Pune- 411 021 & Lecturer, Department of Computer Science,
Government Art and Science College, Veerapandi, Theni -625, Tamilnadu, India

**Dr.V. Isakkirajan Ph.D**
Assistant Professor (HOD), Department of Computer Science,
P.K.N Arts & Science College,
Tirumangalam-625 706, Tamilnadu, India

**P.Senthil Kumaran**
Lecturer, Department of Computer Application, Government Art and Science College,
Veerapandi, Theni -625 534, Tamilnadu, India

## ABSTRACT

*The structure of waviness on the functioning surfaces of behavior parts is connected through fluctuations in the mass of the hack coat of metal and changes in the mechanism of the wounding might. Laplace operators were used to replica the hub fewer grinding scheme based on the edifice of the relocate purpose and the feature equation. It was establish that the structure of waviness depends on the position of the hodograph of the movement of the vector of the hub of the part in the multifaceted aircraft, which in revolve depends on the numerical parameters of the firm handcuffs of the hub fewer dicer appliance. This makes it probable, based on hodographs and the bony direction of their asymptotes, to decide the numerical steadiness of the method depending on the angles of alteration of the firm chains of the dicer mechanism Two practical approaches were used to confirm the correctness of the hypotheses. The first one is a multiplication of wave's hodographs.*

*The subsequent single is revival dislocation and the accident of the mutual hood grid of renaissance and waviness dislocation mechanisms with the hodograph of considerably firm appliance dislocation.*

*The diagrams which permit choosing geometry of alteration of rigid hold that allows to augment or decrease parameters of convinced harmonics are urbanized. The 3D illustration allows location the limited minima, characterized by suitable numerical alteration condition, only if keeping pace waviness of the operational surfaces of manner parts.*

**Keywords:** Development Novelty, Alteration, Asymptote, Choral Psychotherapy, Hodograph, Waviness.

**Cite this Article:** Saravanan Suba, Dinesh Senduraja, V. Isakkirajan and P.Senthil Kumaran, Construction of Comportments Quantities Undulation Throughout Hub Rarer Mortise Crushing on Secure Manacles, *International Journal of Information Technology (IJIT)*, 5(1), 2024, pp. 1-23
https://iaeme.com/Home/issue/IJIT?Volume=5&Issue=1

## 1. INTRODUCTION

Through the produce of breaker bearings, the excellence of treated undulating surfaces is necessary [1]. while grinding the practical undulating surfaces of breaker behavior charms, it is essential to make sure speedy exclusion of grant and lofty meting out recital, the concluding universal-and micro numerical correctness of the treated outside, and fulfillment with corporeal and automatic necessities [2]. The dimension of the slash coat through grinding is relative to the standard grinding might [3]. The structure of the waviness of the information is caused bydeviations in the mass of the cut sheet or changes in the grinding strength [4]. exterior coarseness depends on the fabric of the division and the grinding controls, the efficiency of the stipend exclusion, and the relation rate flanked by the fraction and the grinding helm. The

Grinding strength is the chief changeable for the machiningprocedure psychiatry [5].

The system of the go-ahead replica, which was worn to forecast together stationary (arithmetic) and active steadiness of the procedure of hub fewer grinding on firm chains, is revealed in Figure 1. through the hub fewer grinding courserevise, the peripheral strength vectors of manacles *A* and *B* were not measured since they contain minute principles and do not considerably influence the modeling. The machinery of the grinding military $Fn$, $Ft$, attractive into description the strength$FG$ arising beginning the burden of the division and the force $FM$ from compelling preservation, form the organization of strength vectors of the reactions of the chains $FA$, $FB$, which is required to guarantee the inert equilibrium of the grindingmethod. As seen in Figure 1, the hub of the division isshifted relation to the hub of the hold up by a minute sum ($\Delta X$; $\Delta Y$). This is complete to make sure enduring phone with the handcuffs of the part. One of the chief Parameters of the hub fewer grinding development that can be forbidden is the angles of proclivity of the chains ($\varphi 1$ and $\varphi 2$).

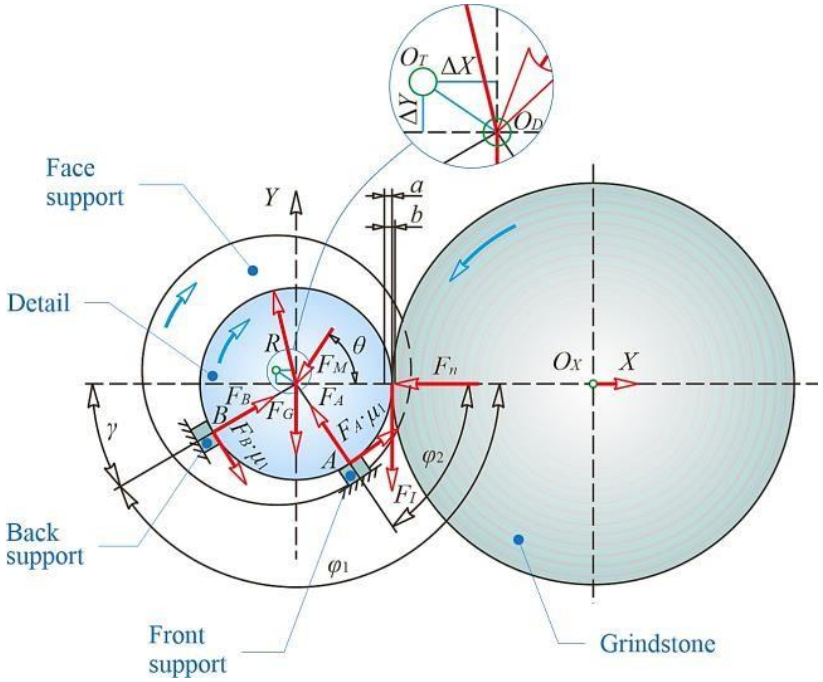


**Figure 1 –** system of a go-ahead replica for predictingthe constancy of the hub fewer grinding [6]

That is why construction requires recommendations for choosing the charge of the angles of the cuffs and obtaining the closing in time harmonics, gratitude to this. though, such recommendations entail investigate and technical good reason of their outcome [6].

## 2. LITERATURE REVIEW

To investigate the grinding processes, there are arithmetical models worn by Laplace operators toexamine the hub fewer grinding method. The study of the transport purpose and the answerof the feature equation is approved out with chart- logical methods [7]. The structure of wavinessdepends on the location of the hodograph of theassociation of the vector of the hub of the feature in the compound airplane, which in revolve depends on the arithmetical parameters of the firm chains of the grinder mechanism[8, 9]. alteration angles $\varphi 1$ or $\varphi 2$ directly shape the standard module of grinding strength, wounding deepness, steadiness in the hurtful district, and, thus, the harmonics of the recently shaped waviness of manner particulars [10].

In the Laplace district, growth is compulsory tounite the instrument of waviness and the apparatus of renewal. For graphical psychiatry the apparatus of the mutual outcome is resolute by multiplying the vector by the matching worth of $s = \sigma + jn$. In this container, the organize cause vector for together swell and renewal mechanisms is at the identical occurrence and $\sigma$ (here, $\sigma = 0$). In vector growth, the standards of both vectors are multiplied, and angles from the optimistic genuine axis are additional. For instance, Figure 2 shows the vector's development at a incidence of $n = 7.5$. The waveform has a scale of 2 and an viewpoint of -45°, and the rebirth vector has a extent of 3 and an viewpoint of 120°. The mutual vector for this situation is exposed in Figure 2b, where the value of $n = 7.5$ is the vector6 (2, 3), and the approach is 75° (120° + (–45°). The fraction of the hodograph of the choral vector 6to 8 shows the universal depiction of the mutual hodographof the vector for dissimilar harmonics and circumstances place up. rudiments of the example of the mutual process of the hodograph instrument from the 2nd to the 10th choral beneath a precise debugging situation [11].

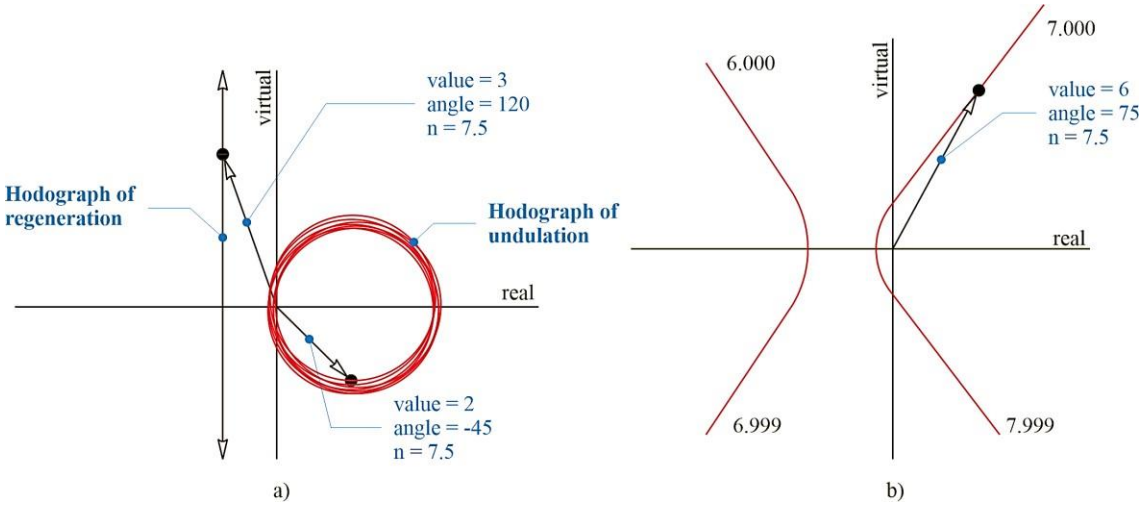


**Figure 2 –** Vector growth scheme (a) and collective hodograph of the vector from 6th to 8th harmonics (b) [6]

These forms of hodograph hyperbola are intense approximately a point (–0.5; 0) in the multifaceted plane and have endless asymptotes jacket the variety from 0° to 360° (Figure 3).

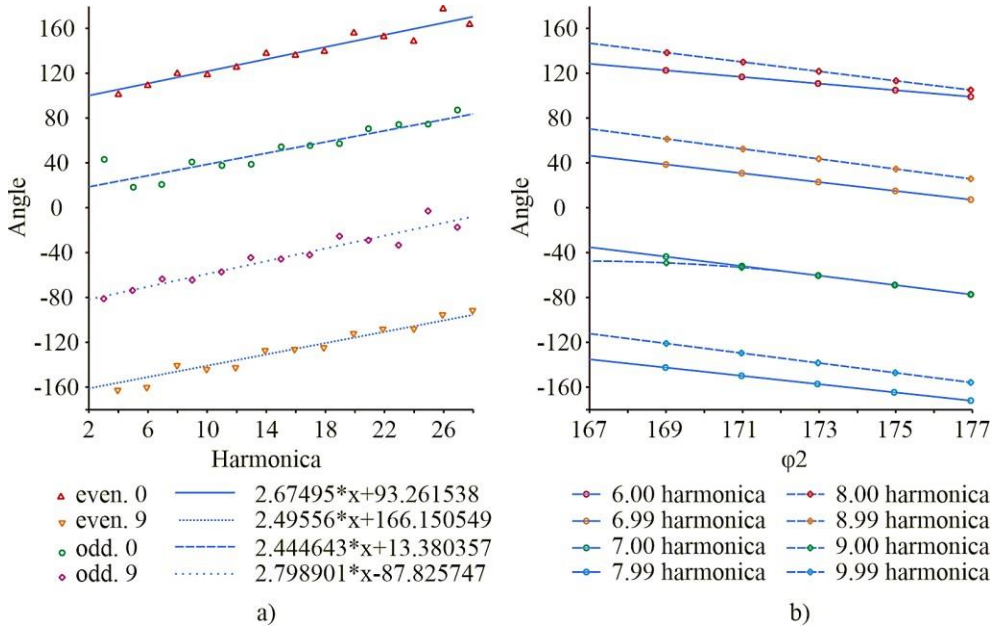


**Figure 3 –** Vector development method (a) and collective hodograph of the vector from 6th to 8th harmonics (b) [11] Asymptotes have fantasy mechanism, preliminary with optimistic perpetuity for integers numbered harmonics (e.g., 5.000, 6.000) and finish with unhelpful perpetuity for statistics of slighter integers (e.g., 5.999, 6.999). It is recognized that the mainly erratic for these hodographs is the rangy direction of the asymptotes. This confirms that the asymptotes roughly 0° indicate the arithmetic unsteadiness of the procedure [12].

## 3. INVESTIGATE TACTIC

We will examine the modify in waviness harmonicsdepending on the geometry of the complex of dense manacles (Figure 3a). The asymptotes augment by 2.5° per vocal with still and strange, alliance at just about 180° from every additional [13, 14]. Outline 3b shows the trends of the asymptotes of the angles with a modify in the viewpoint $\varphi 2$ for a little harmonics if the position of the facade hold up is stable $\varphi 1 = 55°$.

This chart shows a diminish in the asymptote of the approach if $\varphi 2$ is augmented. It is also likely to observe still and strange, complete, and after that-to-entire asymptotes of angles around 180° apart. because the asymptotes of angles are obvious array, we require the explanation of angles to clarify the geometry of hub fewer grinding processes [15, 16]. The learn proposes to use two methodologies. The

First is the increase process of hodographs of waviness dislocation and renewal. The subsequent is analyzing the lifelike chance of the mutual hodograph of renewal and waviness associationmechanisms with the hodograph of markedly firmmachine pressure group [17]. The psychiatry showed that the dislocation hodograph has a unhelpful real part, so the apparatus of the waviness upshot on the process is uneven [18]. At the similar occasion, the approach of such hodograph group of the waviness machine will obtain a worth better than 90° or less than -90° from the optimistic genuine alliance. because the hodograph of the group of the renewal machine is in a convinced district, the viewpoint of the hodograph will be comparable at a agreed incidence. If the waviness and renewal mechanisms match at a convinced numbers (arithmetical angles are salaried), the mutual dislocation hodograph forms a hyperbola with an asymptote of 0° (-360°). Sucha recompense instrument indicates the numericalunsteadiness of the asymptotes for several harmonics [19].

For an considerably firm appliance, the hodograph of dislocation in the multifaceted airplane is positioned at the end at the cause of the coordinates. At the identical occasion, the hodograph of waviness association and renewalenters the region approximately the point (–0.5; 0). The dislocation hodographs, which have an asymptote near 0°, typically interconnect with the mechanism dislocation hodograph. The fact that the consequences fall in the proposal of the progression instrument equivalent to the communication for this indicated occurrence of the undulation allows the enlargement of this choral due to volatility in thedispensation region [20]. The agreed explanation involvesan markedly solid mechanism, so the revise points to the arithmetical volatility of the waviness incidence, which consists of a vector accident in the multifaceted hydroplane. It has been recognized that the asymptote angles mainly depend on the figure of harmonics and the geometry of alteration angle, so it allows for predicting which harmonics will be unhinged in a specified choice of alteration angles [21]. believe a convinced angle of the asymptote of one choral is distorted and investigated through the full compound of alteration geometry. In that container, it is experiential that the academic geometric unsteadiness of the particular numeral of harmonics will apparent if the asymptote's position is a manifold of the worth in radians – $2\pi$. through the investigate, a curve diagram of the asymptote viewpoint was obtained, and the 14th harmonics were deliberate insidethe normal geometry of hub fewer grinding on solid chains (Figure 4).

The rangy budge beginning $2\pi$ to 0 radians leads to a elevated thickness of contours, allowing one to observe chairs where the asymptotes are multiples of $2\pi$ effortlessly. This graph shows that the 14th choral is hypothetically uneven at $\varphi 1$ = 52°, 78°, and $\varphi 2$ = 143°, 168°. though only single line in every of these regions will be precisely 0°, instability ripples are ordinary for harmonics whose statistics are absent from the entire due to a chapter move in the rebirth of waviness renewal throughout grinding. consequently, looking simply at the universal district, where the complete choral is wobbly, is greatest. For example, in Figure 4, an ellipse can be pinched roughly each area of the rigorous curve lines to signify the foremost zones where 14th harmonics are theoretically unstable. psychiatry of shape 5 makes it probable, with elevated prospect, to foresee the arithmetical shakiness in the wounding district during grinding, thereby predicting the enlargement or decrease of a choral wave.

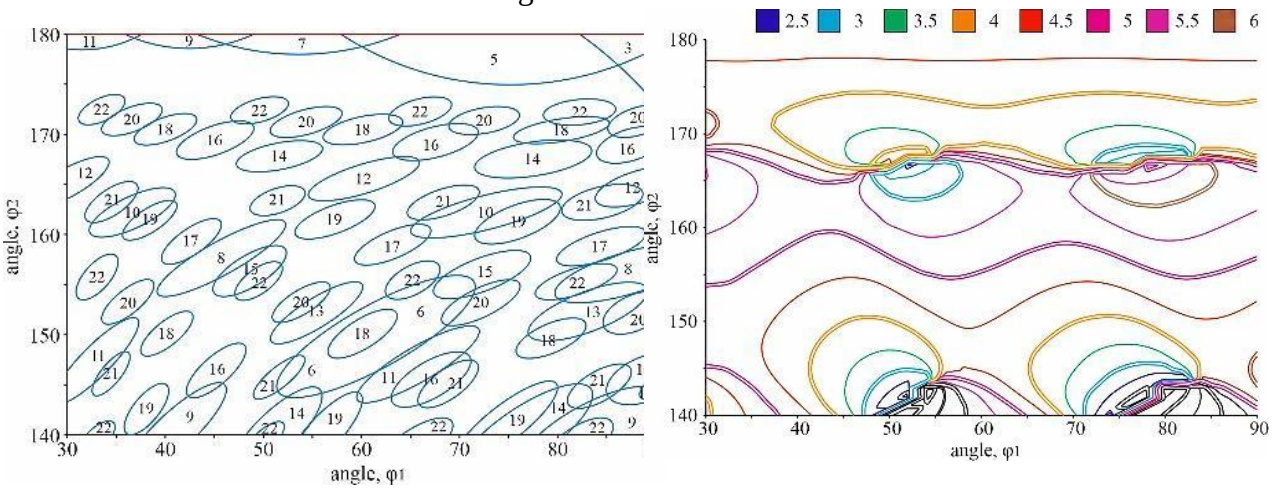


**Figure 4 –** The arithmetic volatility wave figure constructed with rangy psychiatry of the mutual dislocation hodographat the constancy limit within the distinctive clear up geometry

Wireless sensor networks (WSNs) consist of a number of static or mobile sensors in self-organizing and multihop man-ner, aimed at sending the information detected and processedby the sensor nodes in the coverage area of the network to theusers [1, 2]. WSNs integrates MEMS, sensor technology withnetwork communication technology [3] and is widely used in agriculture [4], military [5], environmental protection [6],intelligent transportation [7, 8], and other fields. It has been the focus and highlight of international competition because of the focuses of Industry and Academia [9, 10].

Because the location information of nodes plays an important role in the working process of WSNs [11], local- ization is an indispensable basic technology [12]. Although the current GPS localization system can accurately locate the target, it is difficult to use satellite positioning information for accurately locating the target in some special places [13, 14]. Therefore, it is very meaningful and challenging work to study the accurate localization algorithm for WSNs.The rest of this paper is organized as follows: In Section 2,

we describe the localization algorithms in WSNs and the main contributions of our work. In Section 3, we improve the Archi-medes optimization algorithm (AOA) and compared with the other algorithms. In Section 4, the MAOADV-Hop localiza-tion algorithm is proposed and the the experimental simula- tion comparison is carried out to verify the performance of the localization algorithm. Finally, we summarize the work of this paper and describe the future work in Section 5.

The range-based localization algorithm mainly included RSSI [16], TOA [17], TDOA [18], and angle of arrival (AOA) [19]. The range-free localization algorithm included centroid [20], weighted centroid, DV-Hop, amor- phous [21], and APIT localization algorithm [22]. The posi-tion accuracy of range-free localization algorithm can satisfymost of the needs, which is popular among users [23].

The DV-Hop localization algorithm is one of the most famous range-free localization algorithms in WSNs [24–26] due to its high robustness and simplicity. But, the DV-Hop algorithm has a lower localization accuracy incomplex environment. Thus, many improved DV-Hop algo-rithms have been proposed in recent years.

Messous et al. proposed an improved recursive DV- Hop localization algorithm for randomly deployed wireless sensor networks, which uses an optimization formula tocalculate the average hop count of anchor nodes to obtain better localization accuracy [27].

Shi et al. proposed an improved DV-Hop scheme based on path matching and particle swarm optimization algorithm, which uses an improved particle swarm optimization algorithm to optimize the location of unknown nodes [28]. Han et al. pro- posed an improved localization algorithm based on the improved DV-Hop and differential evolution (DE) algorithm in 2020 [29]. Huang and Zhang proposed a weighted DV-Hop localization algorithm for wireless sensor networks based on DE algorithm [30]. Lei et al. pro-Compared with DV-Hop, DE_DV-Hop, and BOA_DV- Hop, the MAOADV-Hop has better convergence rate than that of DE_DV-Hop and BOA_DV-Hop and has better localization accuracy than that of the DV-Hop and BOA_ DV-Hop.

# 4. AOA AND MAOA

In this section, Section 3.1 introduces the entire optimization process of AOA. Section 3.2 improves AOA by using the tent chaotic map and the concepts of social learning and individual cognition in PSO, and MAOA is proposed. Sec- tion 3.3 verifies the performance of MAOA by comparing with five swarm intelligence optimization algorithms.

***1.1. Archimedes Optimization Algorithm.*** AOA is a meta- heuristic algorithm inspired by Archimedes' principle. Like other population-based metaheuristic algorithms, AOA begins its searching process through an initial population with random volume, density, and acceleration. The steps of the algorithm are as follows.

***Step 1. Initialize population position, volume, density, and acceleration using***

$X_i = \mathrm{lb}_i + \mathrm{rand} \times (\mathrm{ub}_i - \mathrm{lb}_i);\ i = 1, 2, \cdots, N, \mathrm{acc} = \mathrm{lb} + \mathrm{rand} \times (\mathrm{ub} - \mathrm{lb});\ i = 1, 2, \cdots, N,$

sparrow search algorithm (SSA) in wireless sensor net- works in 2020, using the double communication radius method to improve DV-Hop and the improved sparrow search algorithm to estimate the location of nodes [31]. Huang et al. proposed a three-dimensional localization algorithm for WSNs based on improved A∗ and DV- Hop algorithms [32]. Han et al. proposed a multitarget vector hopping localization algorithm based on differential

$\mathrm{den}_i = \mathrm{rand}(N, D), \mathrm{vol}_i = \mathrm{rand}(N, D)$, where $X_i$ denotes the $i$th object in $N$ population. $N$ and $D$, respectively, denote population number and

dimensions of the search space. $ub_i$ and $lb_i$ are the lowerand upper bounds of the search space, respectively. evolution quantum particle swarm optimization

The main contributions of our work in this paper can besummarized as follows.

The Archimedes algorithm is optimized. Firstly, tent cha-otic map is introduced into AOA to increase the diversity

of social learning and individual cognition in PSO are

the $i$th object, respectively. rand $N, D$ is a $N \times D$ dimensional matrix, which can be randomly calculated by the system function. Then, the individual $X_{\mathrm{best}}$ with the bestfitness value and the corresponding $\mathrm{acc}_{\mathrm{best}}$, $\mathrm{den}_{\mathrm{best}}$, and

$\mathrm{vol}_{\mathrm{best}}$ were selected.

***Step 2. Update the density and volume of $t + 1$ th iteration of ith object using***

$$\mathrm{den}^{t+1} = \mathrm{den}^{t} + \mathrm{rand} \times (\mathrm{den}_{\mathrm{best}} - \mathrm{den}^{t}),$$

## 4.1. Autism spectrum disorders

monitoring of depression have been investigated in [5, 6], in order to reduce misinterpretation of the diagnosis.

To this end in [5], a wristband was designed using ICT for daily data collection and analysis from depressed patients. A mobile detection solution to assess students' mental health, has also been proposed in view of the depression rate increasing on university campuses.

### 4.2. Bipolar Disorder (BD)

Bipolar disorder (BD) is a serious mental illness thataffects 2.6% of the US population aged 18 years and older per year. As rhythmicity is a key component of well-being in bipolar disorder, it has been assessed using smartphones for automatic detection [7]. Dynamic psychological processes (bipolar disorder) are most often assessed using self-report instruments [8, 9]. Their limitations have been assessed through the use of smartphone sensors, in which clinically validatedtreatments have been previously incorporated, as anacquisition system [8]. However, the status of patients with bipolar disorder can be classified using information collected by Smartphones [10].

### 4.3. Attention-deficit / hyperactivity disorder(ADHD)

According to [11], ICTs are used to establish diagnosis and monitoring of students between 6-18 years old with Attention-deficit/hyperactivity disorder (ADHD). Advanced ICT tool as Gordon Diagnostic System (GDS) has been used for assessment and diagnosis. And Learning Management System (LMS) has been used to address special need of students with ADHD learning abilities and preferences. However, other ICT solutions for ADHD students helping exist such as: online learning and augmented reality based education. But, more research is needed to evaluate the different proposed solutions.

### 4.4. Dementia and ICT

According to [12], UN statistics show that our society is ageing rapidly, leading to an assistive technologies development increasing, for people with dementia.

Policy makers (politicians and governments) are concerned about the contribution of technology to the effective management of people with dementia. According to World Health Organization (WHO), 1 of 160 persons in the world is diagnosed with Autism Spectrum Disorders (ASDs). However, in low-and middle-income countries (LMIC), the prevalence of ASDs is partially unknown or properly investigated.

The review pointed out a series of ongoing projects or already archived. For example, in [14, 15], the authorsworked on a project to discover the link between avoidant personality disorders (APD) and, physical and psychological stress. A test was conducted on two samples, one composed of patients with avoidant personality disorders and the other of healthy people.

### 4.5. Early detection of mental illness

Machine learning techniques have greatly contributed to the development of tools to assist doctorsin mental disorders prediction, in particular anxiety disorders. The study reported in [16] concerns the early detection of mental health changes in individuals by combining passive smartphone sensors with the Cross Check method. In this case, the disease of schizophrenia is concerned. Many other ICT-based toolshave been used for early assessment of other mental illnesses, such as wireless sensor networks (stress), wearable biosensors (bipolar disorder), mobile phone platforms (stress and physiological arousal) [17],acceleration and voice intensity sensors (behaviour andcorrelation with mental health), smartphone sensing (bipolar disorder, depression), semantic web (autism), etc.

### 4.6. Affective illness

Affective disorders are frequently encounteredamong elderly populations. Sleep disturbance is a common and important component of affective illness. The SWOT (Strengths, Weaknesses, Opportunities and Threats) analysis method was used to measure ICT impact on affective disorders' diagnosis in older people.The idea was to see if there would be any added value in using these techniques in addition to traditional clinical diagnostic methods. It was found that ICT offersinteresting tools for affective disorders diagnosis and management, but seems to be poorly known by practitioners and future users [18, 19].

### 4.7. Autonomy loss

According to [20], the use of ICT can provide addedvalue in frail elderly people monitoring, and could potentially contribute to reduce the risk of institutionalization. To this end, a Safe and Easy Environment (SafEE) project has been developed to improve the elderly's living conditions. It combines an ICT-based behavioral analysis platform with adapted non-pharmacological therapeutic responses. The resultsshow that the platform has been accepted by all stakeholders [20].

### 4.8. Schizophrenia

Human behavior is increasingly being reflected or interpreted by sensors and ICT. This is particularly important when it comes to behavioral changes associated with severe mental illnesses, including schizophrenia [16, 21]. Passive smartphone sensors have been used to collect data from schizophrenia patients recently discharged from hospital. This was done to monitor their mental health indicators to facilitate the prediction and early management of relapse. The results show a correlation between different behavioural characteristics (sleep, mobility, conversations, smartphones use) and mental health indicators related to schizophrenia [16].

### 4.9. Parkinson's disease (PD)

The major cause of morbidity and mortality among patients with Parkinson's disease (PD) is the motor changes that restricting their functional independence. Therefore, monitoring the disease manifestations is crucial to detect any worsening of symptoms timely [22,23]. To this end, wearable sensors have been attached tothe feet of patients suffering from it in order to collect and analyze their physiological data. This would facilitate its better monitoring for more effective management [23].

## 5. ALGORITHM PRINCIPLE

The JPEG algorithm is an image compression coding standard formulated by the International Organization for Standardization ISO, which uses lossy compression to reduce image repetition and redundant image data. JPEG algorithm compression mainly consists of four steps: image preprocessing, discrete cosine transform, quantization, and encoding.

### (1) Image preprocessing

When compressing an image, it is necessary to separate the brightness and color, convert the color mode, convert the RGB color model into a YCrCb model, and change the RGB value into a YCrCb value, where Y represents brightness, Cr represents red chromaticity, and Cb represents saturation. The conversion relationship is expressed by the following formula:

$$Y = 0.299R + 0.587G + 0.114B \quad (1)$$

$$Cb = -0.1687R - 0.3313G + 0.5B \quad (2)$$

$$Cr = 0.5R - 0.418G - 0.0813B \quad (3)$$

After conversion, chroma downsampling is performed to reduce the chroma and saturation thatare not sensitive to the human eye.

## (2) Discrete cosine transform

The image is divided into 8*8 pixel blocks, and each pixel block is processed to find out the high-frequency information that is not sensitive to the human eye and process it. The discrete cosine transform (DCT transform) conversion formula is as follows:

## (3) Quantification

After the original image undergoes discrete cosine transform, the next step of data quantization processing is performed. The function of quantization is to delete high-frequency information that is not sensitive to the human eye, and lose part of the accuracy in exchange for less space storage occupation. The quantization algorithm is shown in the formula:

$$K_{ij} = round\left(\frac{G_{ij}}{Q_{ij}}\right) \quad i, j = 0,1,2, \dots ,7 \quad (7)$$

In the formula, G is the image matrix, Q is the quantization coefficient matrix, and the round function is used to round floating-point numbers. The JPEG algorithm uses standard luma $Q_Y$ and chroma $Q_C$ quantization tables for quantization operations. As shown in Figure 5 below:

$$Q_C = \begin{bmatrix} 17 & 18 & 24 & 47 & 99 & 99 & 99 & 99 \\ 18 & 21 & 26 & 66 & 99 & 99 & 99 & 99 \\ 24 & 26 & 56 & 99 & 99 & 99 & 99 & 99 \\ 47 & 66 & 99 & 99 & 99 & 99 & 99 & 99 \\ 99 & 99 & 99 & 99 & 99 & 99 & 99 & 99 \\ 99 & 99 & 99 & 99 & 99 & 99 & 99 & 99 \\ 99 & 99 & 99 & 99 & 99 & 99 & 99 & 99 \\ 99 & 99 & 99 & 99 & 99 & 99 & 99 & 99 \end{bmatrix} \quad Q_Y = \begin{bmatrix} 16 & 11 & 10 & 16 & 24 & 40 & 51 & 61 \\ 12 & 12 & 14 & 19 & 26 & 58 & 60 & 55 \\ 14 & 13 & 16 & 24 & 40 & 57 & 59 & 56 \\ 14 & 17 & 22 & 29 & 51 & 87 & 80 & 62 \\ 18 & 22 & 37 & 56 & 68 & 109 & 103 & 77 \\ 24 & 35 & 55 & 64 & 81 & 104 & 113 & 92 \\ 49 & 64 & 78 & 87 & 103 & 121 & 120 & 101 \\ 72 & 92 & 95 & 98 & 112 & 100 & 103 & 99 \end{bmatrix}$$

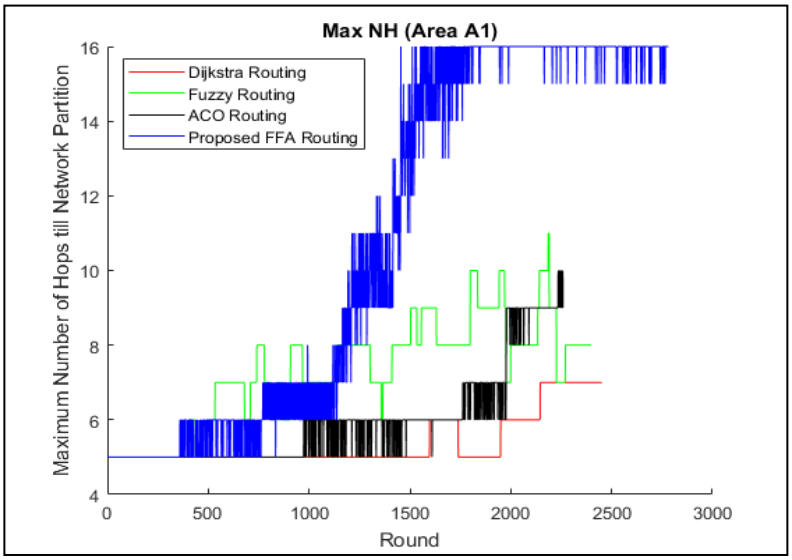


**Figure 5**

## Coding

The difference De of the quantized DC coefficients between adjacent image blocks is encoded, and the formula is:

$$De = (0,0)_i - DC(0,0)_{i-1} \quad (8)$$

Once encoded, the raw image captured by the camera can be compressed into an easy-to-transmit JPEG data stream.

## The role of the algorithm

This algorithm compresses the original image, processes the original video format that is inconvenient to transmit, effectively controls the size of the original image, and uses limited bandwidth to transmit more data. At the same time, it can also reduce the occupation of the CPU computing resources of the development board, and obtain a better video picture, which is conducive to the realization of remote real-time video monitoring.

## Equalization Algorithm

If the brightness value of the pixel in the image, that is, the gray level, is regarded as a random variable, then its scattering characteristics reflect the statistical characteristics of the image, which can be expressed as a gray histogram (Histogram). The abscissa in the histogram represents the gray level, and the ordinate represents the number of pixels on each gray level. It reflects the degree to which a picture has information such as different colors or textures within a certain period of time. Therefore, histograms are widely used in fields such as image processing and pattern recognition. This paper introduces the histogram algorithm and its characteristics. and look forward to its development. The grayscale histogram is the basic statistical feature of an image. It has three properties:

(1) The histogram counts the number of pixels of all gray levels, it only shows the number of pixels of each level of gray value, but not the orientation in the picture. In other words, this only represents the number of grayscale values that exist in the image, and the orientation part is discarded.

(2) For any picture, there is one and only one grayscale histogram, but there may be the same histogram for different pictures

(3) Since the histogram is obtained by adding the number of pixels with the same gray value in the image, the histogram of the image is divided into several sub-blocks, and then the histograms of the sub-blocks are calculated separately.

The key point of the global grayscale histogram equalization algorithm (HE) is to map the grayscale histogram of the original image from the area where the number of pixels is gathered to the entire area in a balanced manner. The HE algorithm is a nonlinear transformation method, which re-transforms the gray value and averages the number of pixels in the entire area. This makes the distribution area of the overall gray domain larger, that is, the contrast of the entire image is improved. Because the HE algorithm is widely used in the field of airspace enhancement, it has many research directions and obvious effects. The most important thing is that it has the characteristics of fast operation and meets the real-time requirements on the

Eembedded platform. Therefore, the HE algorithm is used in this paper. The specific contents ofthe global HE algorithm are as follows:

First record the number of pixels at each gray level, and then record the normalized histogramof the image.

$$h(r)=n,k =0....55 \quad (9)$$

In the above formula, the picture has a total of 256 gray levels, k-=0,1...255, r is the k-th level gray value, and nk is the number of times the gray level k is represented in the picture. It can be obtained from Equation 9:

$$p(rk)=\frac{nk}{W*H} \quad \text{——}, k = 0,1,\dots\dots,255 \tag{10}$$

In the above formula, W and H represent the size of the image, that is, W*H represents the total number of all pixels in the image, and p(rk) represents the probability that the pixel whose gray value is r appears in the image, that is, the image is classified as -- The grayscale histogram after transformation.

Find the cumulative distribution function.

$$T(rk)=\sum_{j=0}^{k} p(rk) \tag{11}$$

Rounded and expanded:

$$T(rk)=int[((n-1)-0)*T(rk)+0.5] \tag{12}$$

$\sum_{j=0}^{\kappa}(rk)$ is equivalent to the cumulative addition of the probability that the gray level is 0~k

in the image, and T(rk) represents the cumulative distribution probability of the gray level rk. Equation 11 is also known as the cumulative distribution function of the image.

Obtain a corresponding grayscale lookup table by accumulating the distribution function, and then replace the pixels in the original image with the corresponding grayscale values in the lookup table.

$$Sk = 255xT(rk) \tag{13}$$

In the above formula, Sk represents the gray value in the image after the image has been mapped, and the global gray histogram equalization can automatically enhance the contrast of the overall image.

The optional steering etiquette include firefly algorithm. The reason of this method is get to vigor intense poise to environ maximization of net lifespan. Firefly algorithm is hired to figure best method for transmitting details from feeler lumps to fall. In this thesis we assume a forecast that mimics time vigorsteering. This means every lump can propel cartons to fall by best trail in time cycle. Via this agenda, the best route willpower linking transfer factscartons for total lumps is reduplicate in also about The submitted method logy involves set region scope. The lumps are aimlessly deployed in this pasture. whole lumpshave full information as to their locations and national's locations under transfer reserve furthermore spot of foot class. The utmost show variety and the original vigor are alike for full lumps.

Competence and dependability of energy course are the most WSNs plan challenges. running vigor fatigue stand for a vital confront for WSNs plan.It awards the network lifespan which is the nearly all large metric for WSNs estimate. We can name the net lifespan,era from net begin operation until first feeler drain its control. The lifespan is the intense design insolence in WSNs. One of the sizeable techniques that is worn to maximize lifespan is by rising network steering algorithm.

This thesis submits a urban steering algorithm. The future steering utilized by via two metrics. Theinitial is lump remaining vigor, and the next is the direct hop to fall. The submitted algorithm taking charge of determining the optimal route from lumps towards fall and ensuring balancing vigor consuming. opposite vigorfatigue leads to expand network lifespan. So, the optional steering technique involves ruling the best route that ensure lumps vigor fatigue balance.

The total makeup of the submitted apology is established byin fig. 1. The submitted method logy acts as facts that folcowers. In time a lump want transmits cartons near fall, the algorithm collects all nationallumps firstly, and by a machine it finds the viable lumps (FN) for every feeler lump and gather back the awful ones. The viable national lumps would give a share in final process that chronic optimum route for broadcasting

The prospect algorithm compute purpose tax for possible lumps. According these standards, the algorithm selects thepossible lump that grade do well tempo for selecting as then jump. Then unite it keen on OPT list through in similar time ensign it equal for present lump. The submitted method later checks the present lump insomuch as byin foot position region. factual container makes course end by best methodthe same to OPT list. bogus box makes present single is then use submitted method logy for willpower next best lump to propel carton. The submitted means reiterated for every one longing drive details. The algorithm selects the lump that has peak chance value planned via the robustness role.

Yang [16] is the initial who inserted Firefly algorithm. This method simulates the contact of fireflies via theirflashlight. All fireflies are unspoken as unisex in this algorithm. This denote that any firefly can involved by any firefly depending on others intensity. The algorithm is affirmed be crouch.

cartons. possible lumps lost in which at slightest ans that there is no trail for sensing details cartons and network divider has been reached. possible lumps are selected as the adjacent lumps to the fall by stare to present lump. The submitted algorithm uses the firefly algorithm to locate the best trail from lumps to drop by utilizing two metrics, the lingering vigor and straight hop to fall. firefly algorithm involves via two metrics, glow strength and coldness to added fireflies. In the outlookalgorithm beam power will symbolize left over vigor (RE)and reserve (SH) will correspond to the reserve of lumps to thedescend. transfer essentials carton will symbolize firefly's society from solitary to a different chance form job takes into reflection these two metrics. The fol cowering health purpose is prospect and is careful in the imitation.So, the algorithm determines highest probability value fromthe feasible lumps (FN) and select its lump to propel facts cartons (which signify the group of a firefly to an additional).The intended firefly algorithm [16]start

## Object Purpose

Generate an initial population of fireflies (representscattered lumps in the zone region)

Formulate light intensity I so that it is associated by (light intensity (attractiveness) represent lump residualvigor)

Define absorption cocapable  While (t<MaxGeneration)

For i=1:n (all n fireflies) For j=1:I (n fireflies)

If ( ),

Vary attractiveness (RE) by distance r(SH) via move firefly I towards J;

(Represent distance from lump to fall (SH) and (RE) andfind best f(n) value)

anywhere; w1 and w2 are the weights for used metrics, RE isthe remaining vigor, SH is the shortest hop, n is thepresent lump, N is the total number of viable lumps (FN). This meaning is careful for looking for best next skip forthe present lump.

Firefly bug make flashes for little time out of a course called bioluminescence. It is linking the charisma of probable victim or equal as well as for the stuff of angle rancid

Rank fireflies and find the current best; (find the optimumtrail)

End while

$^{ij}\ (X_j - X_i) + \alpha_t \epsilon_i$ (2)

1) Fireflies of any femininity could build charisma forextra firefly. 2) An charisma issue is careful whichincline on brilliance of the sparkle, so as fireflies shift towards more beautiful ones. 3) The vividness of fireflies is designed during an object purpose. In this formulation, the left over vigor is recognized to the fine looks. Where; $X_i$ is the initial inhabitants of fireflies, r is distance,

 is the light combination co capable, is the charm,

 is a randomization stricture, is a vector of random numbers drawn from a Gaussian

sharing or reliableallocation

## 6. EXPERIMENTAL SETTING

Imitation is achieved by via MATLAB. A 100mx100m topological region district is second-hand in the imitation. A 100 arbitrarily dotted lumps for the topological region district. The topological region has single permanent drop by location of (90mx90m). both lump labor by do well broadcast aloofness amounting to 30m. all lump starts by early vigor amounting to 0.5J. The old worth of carton span is amounting to 200-bit. The jump add up bound has the price of 15 hops. The standards of w1 and w2 are 0.2 and 2, correspondingly. The primary order broadcasting paradigm submitted via [17] is used for imitation as fold cowers:

$$E(pkt_{length}) = E_{elec} * pkt_{length} \quad (3)$$

$$E(pkt_{length}) = E_{elec} * pkt_{length} \quad (4)$$

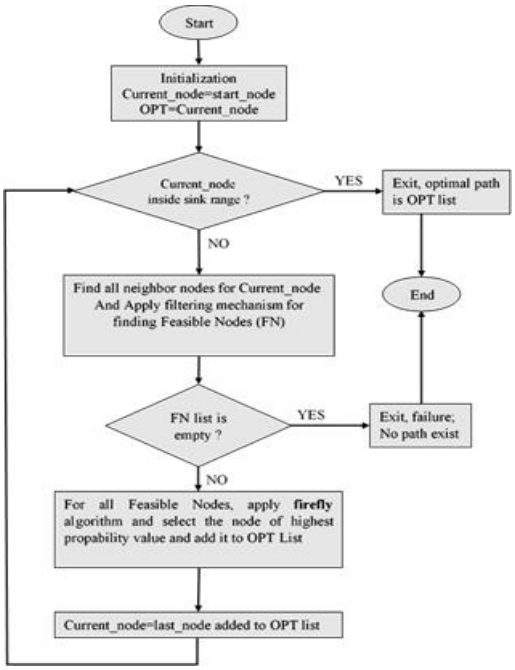


**Fig. 6.** Zone Region A1 of scattered lumps.

Table I clarify cipher for this model. To assess this steering method pack release relation (PDR)has been concerned. Steering etiquette is first-class by PDR is extra than 0.96 percent. The PDR can be intended via the fold cowering equation [13,14].

$$\text{PDR: } = \frac{No.\ of\ Successfully\ delivered\ Packets\ to\ Sink}{Total\ No.\ of\ Packets\ Sent}$$

**Table I** Representation of Paradigm Symbols

| SYMBOL | REPRESENTATION |
|---|---|
| ETX , ERX | Power depletion for broadcasting data,send and receive |
| pktlength | No. bits for either carton |
| *Eelec* | Per bit power depletion, set to 50nJ/bit |
| *Eamp* | Per bit per meter square power depletion,set to 100pJ/bit/m2 |

Figure 7 demonstrates network lifespan by stare to together zones till network divider. The figure. shows that the prospect steering algorithm beat Dijkstra, Furry, and ACO methods. besides, demonstrates maximization by lifespan identical to 2781 about by PDR 0.993. while Dijkstra steering grade 1001 around by PDR 1, furry steering grade 1932 around by PDR 1, and ACO steering rank 2259 around by PDR 1. around is example of juncture that all lumps send cartons to fall. Furthermore, finest follow is reached and vigor use is fair for the optional FFA steering technique. Network divider is speedy forDijkstra steering owing to the employ of similar trails. furry and ACO methods engage impartial vigor fatigue but panel juncture is fewer the optional FFA steering. And this demonstrates the enhancement of the outlook steering algorithm. Table II states lifespan, divider juncture, by PDR for fallout and for the four submitted methods.

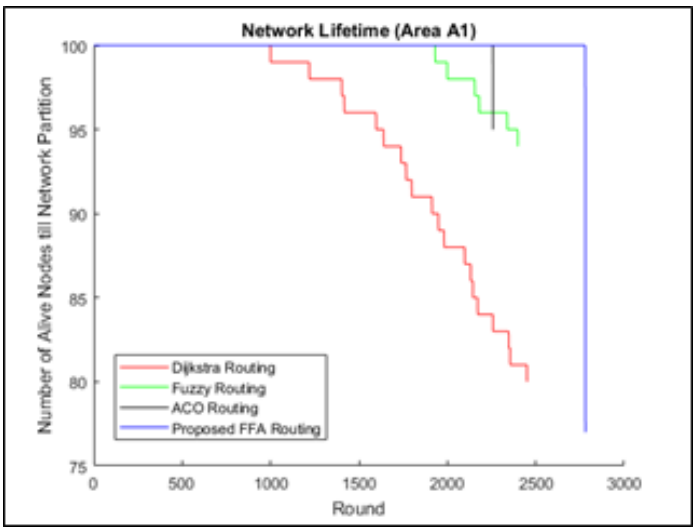


**Fig. 7.** Network lifespan

Figure 8 demonstrates remaining vigor for the compared steering algorithms for the submitted regions. The optional FFA steering algorithm has lingering vigor cowerter than the supplementary methods due to use of further lumps and vigor use guide to poise. And this reflect vigor use is Dijkstra steering is not impartial. furry and

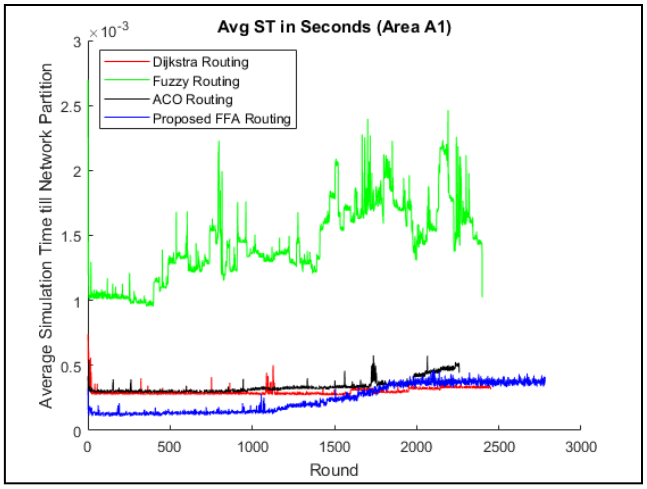


**Fig. 8.** Rate of residual vigor.

Figure demonstrates the standard inspired vigor. Theoptional algorithm consumes extra vigor than Dijkstra,Furry, and ACO methods owing to the able in vigoruse poise. Network panel juncture hold up thiseffect, as the network partitioned extra than juncture for the prospect algorithm. And this improves the optional idea. Figure 6 demonstrate the carton liberation relation (PDR) thatgive the sense of how lots of victory cartons that the fall established the optional algorithm shows a PDR value ofabout 0.993 for the zone region. even though the harmony PDRworth for Dijkstra steering, Furry Steering, and ACO steering but the lifespan augmented in the optional algorithm andbeats the supplementary three methods.

Figure demonstrates hops do well figure that occupied by network. Bin this figure, prospect algorithm involves custom of extra hops for assuring vigor poise and this fallout in lifespan maximization. This form demonstrates the do glowing integer of hops for the optional FFA system is superior the added three methods, and this is how the optional scheme acclimatize itself and share out vigor use on more lumps for construction vigor use poise as mentioned sooner than.

Figure demonstrates networks imitation juncture imitation juncture for the prospect algorithm is fewer than the additional three steering methods, and this prove that this optional algorithm does not influence the process of best track totaling. And this demonstrates the capability for realizing the optional FFA methods in realistic feeler lumps networks. And also, this ensures that the cower potentialfeeler lumps hardware can procedure this steering algorithm inease.

**Table II** Network Throughputs

| Steering Method | Zone | Lifeoccasion | Partition Occasion | PDR |
|---|---|---|---|---|
| Dijkstra Steering | A1 | 1001 | 2452 | 1 |
| Furry Steering | A1 | 1932 | 2400 | 1 |
| ACO Steering | A1 | 2259 | 2260 | 1 |
| Suggested FFA | A1 | 2781 | 2782 | 0.993 |

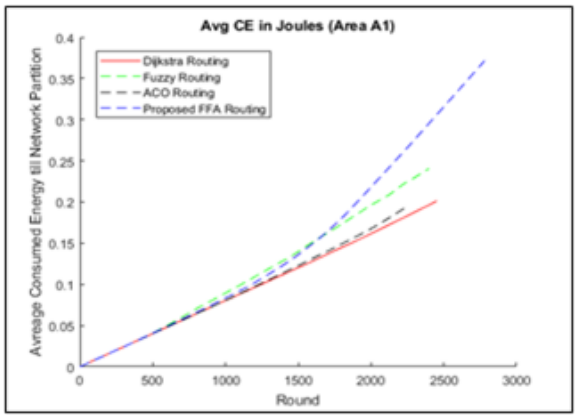


**Fig. 9.** Rate of consumed vigor

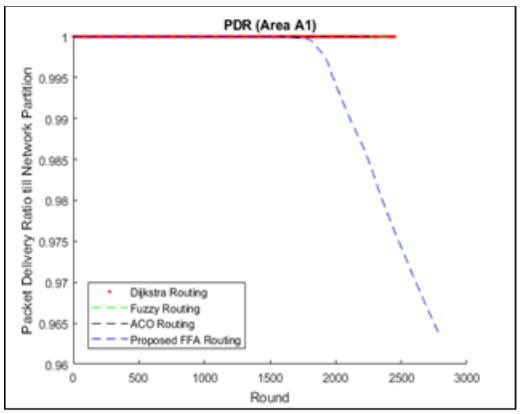


**Fig. 10**. Rate of simulation occasion

Wireless feeler networks involve cower control capital in their life round. The process of maintaining vigor use via innovative steering algorithms meet critical matter. This thesis proposes a firefly navigation algorithm to make certain vigor use poise andgenerally vigor safeguarding so as for amplify the lifespan ofthe networks. Two metrics has been used for imitation which are the outstanding vigor and through hop to fall. The proposes algorithm worn network throughputs to preserve vigor fatigue. Outcome offer an development bin lifespan generation to (2781 round) for the zone region. The prospect algorithm is compared by traditional Dijkstra steering that has lifespan generation to (1001 round) and some intellectual steering methods like Furry steering that has lifespan generation to (1932 round) and ant colony steering that has lifespan generation to (2259 round). Furthermore, product tender first-rate enhancement of the optional steering algorithm alongside the supplementary three algorithms and can be introduced as one of the good quality steering algorithms that capitalize on lifespan.

## 7. DISCUSSION

The growing ageing of the population and health care costs increasing, require a new paradigm for the world's health systems. They need to focus on the patientand put more emphasis on prevention rather than treatment [7]. In this framework, sensors and ICT are usable tools especially in the field of mental health. Thediversity and lack of consensus in the emerging ICT sector is however, a strong limitation for their use in daily practice [10]. The use of information and communication technologies (ICT) could bring added value in mental illnesses' recognition and assessment [10].

According to the literature, research on ICT and sensors' applications in the field of mental health, datesfrom the last two decades and, for the most recent ones from the last ten years. Thus, several authors haveworked on the subject from different perspectives. Many work and techniques used were developed around projects implemented in Europe, from which some are already completed and others are ongoing. A large majority of ICT applications in mental health are based on smartphones and mobile applications [5, 24- 34].

Many studies have linked human behaviour to mental health [15, 28, 35-38]. They show the close linkbetween mental health and human behaviour. The first concern was the possibility to access the invisible worldof psychiatry and psychology. However, human behaviour's study in real life was an opportunity for access. It is better than traditional meetings, and other methods such as patient-doctor screening meetings, where the patient is interviewed by the doctor. These methods have shown their limitations [39].

Since this possibility has been known, various correlations between different mental illnesses and behavioural patterns have been approached. The most discussed are: stress level, depression, loneliness, epilepsy, mood disorders etc. These are factors that influence different people in their employment, social and associative life. A better perception of ICT applications' progress in mental health has been given in [38-40]. While the future challenges are: big data processing and management, patient's data security andconfidentiality.

## 8. RESULTS

### Crash drawing based on rangy psychotherapyof the hodograph

To preserve the steadiness and qualified pace of revolving amid the part and the grinding controls through the machining procedure, the attractive strength of the end hold up must be identical to or go above the peripheral grinding strength (Figure 1):

Figure 11 – Contour diagram of asymptote angles in radiansfor the 14th harmonic within the classic geometry $FM \geq Ft.$ (1)

The viewpoint of the attractive power request is identical to of hub fewer grinding $\theta \geq arcsin()$. (2)

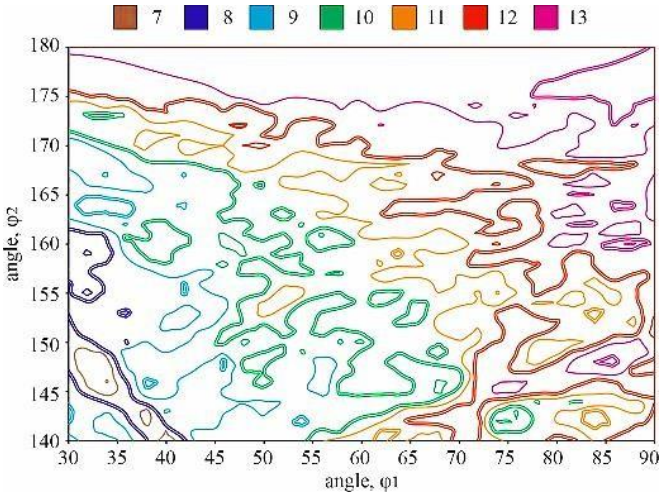


$2 \cdot (\gamma)$

through the examine, fallout were obtained that completeit potential to create a drawing of the numerical shakiness of the waviness for a precise variety of harmonics (2–22) for the typical situation of the geometry of the grinding procedure alteration based on theasymptote angles.

The figure confirms that the hugemass of combinations through alteration of the angles of firm chains are in the county of numerical shakiness,and the instability of harmonics match to a fussy range of standards. For model, believe the 12th vocal, which is geometrically unhinged in the districtof $\varphi 1 = 60°$ and $\varphi 2 = 165°$. The 14th choral is geometrically unbalanced in the district above and to the left next to the principles of $\varphi 1 = 52°$ and $\varphi 2 = 168°$. This plan allows selecting the geometry of the grinding change on firm chains, which increases or decreases the parameters of a exacting choral.

The geometry of the system of firm manacles affects the parameters of the waviness of the operational surfaces of thebreaker manner jewels, and dissimilar angles of the chains have dissimilar belongings on the dissimilar harmonics of the waviness.

while the mutual hodograph of the dislocation and rebirth mechanisms for any choral had an asymptote at 0°, this choral was geometrically unhinged. The angles of the asymptotes followed the major trends depending on the engine's change circumstances agreed this information, it is fair to presume that the earlier the position of the asymptote to 0°, the fewer constant the choral becomes. The synopsis figure is definite as an needle of the quantity of volatility for every debugging situation. When drama this exploit, there is a call for for a limitation that would be relative to theviewpoint of the asymptote, and angles about 0 or $2\pi$ should have a major effect on it, and angle far from 0 or $2\pi$ have small outcome. The cosine meaning satisfies the recognized supplies. If we obtain the principles of the cosines of the radians exposed in Figure 4, the falloutfigure suggests a relation height of shakiness for 14th harmonics under dissimilar debugging situation. In this drawing (Figure 6), contours with levels seal to nothing(0.1, 0.2) are a lot more steady than level roughly 1.0.

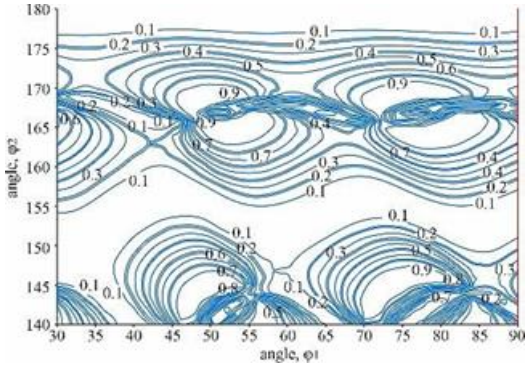


**Figure 12 –** Curve Drawing of Cosines of Asymptote AnglesFor The 14th Vocal Inside The Distinctive Geometry Of Hub Fewer Grinding

If the routine psychiatry is comparable to outline 6 for every choral from 2 to 30 inside the natural geometry of the hub fewer grinding, we find a universal drawing ofthe numerical constancy fallout, shown in Figure 7.

Figure 7 – curve illustration of all cosines of asymptote angles beginning 2nd to 30th harmonics within the archetypal geometry of hub fewer grinding

## Non-nothing sigma, collision drawing rootedin hodograph width psychiatry

If we examine the mutual hodograph of rolling dislocation and renewal with a non-nothing expansion rate, $\sigma$, its graphical depiction change radically. Non-zero $\sigma$ changes the hodograph of renewal association from a in a straight line to a loop. For a constructive $\sigma$, the circle are hued earlier to the point (–1; 0),while the unhelpful σ form circles hued approximately the source (0; 0).

The dimension of the hodograph responds earlier than theexponential purpose so that only at the least changein the value of $\sigma$ does it drastically change the exterior of the mutual hodograph of waviness dislocation and renewal.

shape 8 shows a mutual hodograph of wavinessdislocation and renewal with dissimilar optimistic $\sigma$ from 6.000 to 7.999 harmonics beneath a agreed debugging situation. therefore the hyperbola rotates just about itself, forming recurring spirals. As the sigma value increases, the dimension of the spirals decreases. With an complete augment in the sigma, the dimension of the spirals decrease.

An markedly firm mechanism in the compound airplane is thetop at the source. When the hodograph of the associationof the waviness and renewal intersects with the hodograph of the group of this mechanism, the result isa geometric volatility in the grinding region. If a exacting twisting intersects with the hodograph of the mechanism association, it should be minute sufficient to be close to the derivation. consequently, any worth of $\sigma$ that tin can construct the twisting minute sufficient to cross with the hodograph of the mechanism group will form entity harmonics ofunbalanced height. That is, if one coil is great compared to a new at a convinced $\sigma$, it is obvious that a superior twirl will require a better $\sigma$ to turn into small sufficient to cross with the hodograph of mechanism group. On the additional give, the finest form for grinding will product from the debugging state, the spirals of which form a extremely minute unsteadiness (small $\sigma$) intersecting with the hodographof the mechanism group. Based on this psychiatry, the debugging situation with large spirals is fewer attractive than with slighter spirals at a convinced unhinged $\sigma$. following with these skin tone, an approximation of the geometricsteadiness of the grinder is obtained based on the dimension of themutual hodograph of waviness dislocation andrenewal at steady, non-nothing $\sigma$. If we believe in thecompound hydroplane of the curved of all harmonics under all debugging setting with several non-steady $\sigma$, the whole size of the spirals will be relative to the volatility under each debugging situation. Figure 9 illustrates the amount of the entirety dimension of the spirals from the 2nd to 30th harmonics for each debugging situation inside the standard geometry of debugging hub fewer grinding. A 3D illustration is revealed for the theoretical explanation of explore consequences.

To examine the waviness of the raceways of the behavior rings, it is sensible to use the Fourier sequence, which describes it as a compound episodic purposeconsisting of trouble-free choral oscillations with frequencies that are multiples of the primary one.The succession digit of a effortless choral determines the numeral of irregularities tinted on the part's outside. In meticulous, the subsequent phrase of the Fourier series corresponds to the following vocal and reflectsthe joviality of the fraction's exterior, the third term - the third choral – reflects the trihedral, and so on.

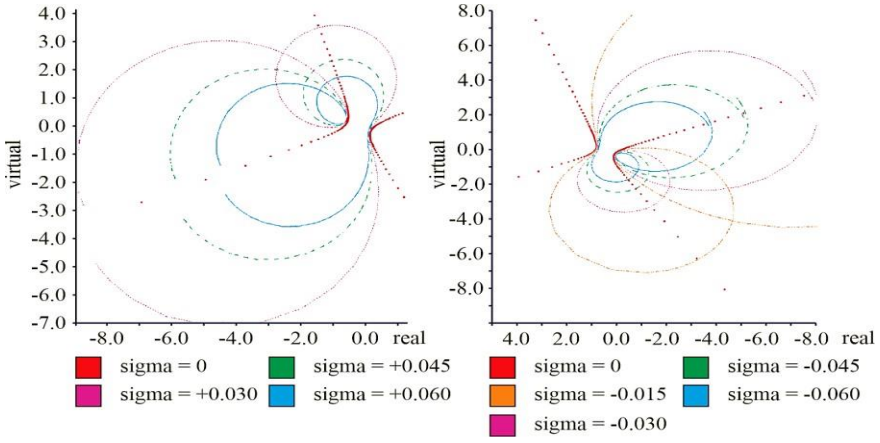


**Figure 13 –** plan of alter of the mutual hodograph of association in a twisting at +sigma (a) and at -sigma (b)

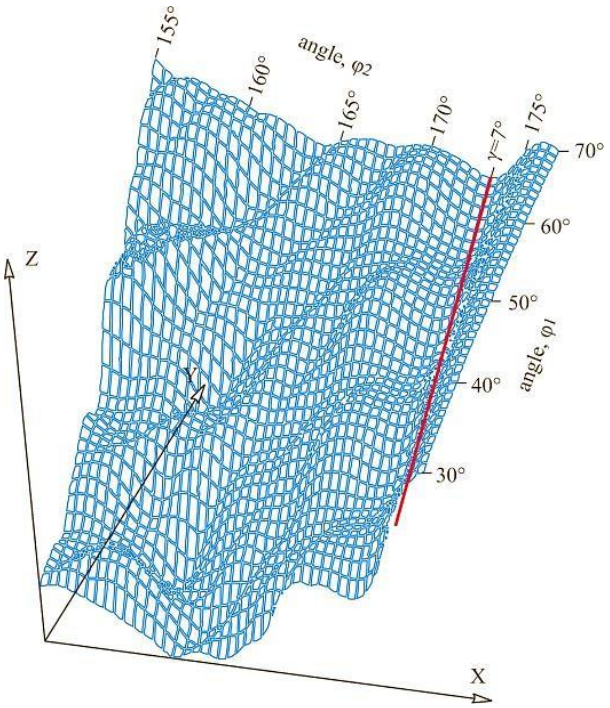


**Figure 14** Format of Modify of The Shared Hodograph of Association In A Twisting At +Sigma (A) and At -Sigma (B)

## 9. CONCLUSIONS

So, as a consequence of the conducted investigate, it was recognized that the individuality of the waviness of the operational surfaces of the breaker behavior jewels are partial by the geometry of the complex of hard handcuffs through hub fewer grinding. It is exposed that dissimilar bear angles during dispensation have dissimilar belongings on the harmonics of the waviness of the operational surfaces of breaker bearings.

The instrument of waviness on the outside of the fraction in the procedure of hub fewer mortise grinding depends on a lot of additional factors (individuality of the grinding controls, mechanism shaking, grinding strength, original and occasion- anecdotal waviness of the fraction), which must be careful to make sure steady excellence.

The geometry of the rigid handcuffs influence the constancy of the hub fewer grinding procedure. The equivalent diagrams illustrate this. In exacting, on the pressure drawing based on the rangy psychiatry of the hodograph, provided that the method finds a steadiness limit $\sigma$ = 0, lesser standards of the alteration angles $\varphi 1$ and $\varphi 2$ lead to superior geometric constancy

In the collision figure based on the lanky psychiatry of the hodograph, beneath a few stage of method volatility, itis also pragmatic that slighter alteration angles $\varphi 1$ and $\varphi 2$ supply superior numerical constancy and ought to lead toenhanced outside coarseness on a energetically steady engine. In exacting, there is a steady restricted despairregarding $\varphi 2 = 173°$ ($\gamma = 7°$), which might be the majority finest form for center smaller quantity grinding. There are quite a few local minima in the illustration, which designate the company of quite a few suitable geometric debugging situation that offer regulated waviness of the element

If the mechanism is animatedly constant from the summit of vision of quivering, then according to the universal drawing of arithmetical steadiness, it is probable to forecast trends of concluding waviness parameters based on the geometry of alteration of firm chains at hub fewer mortise grinding. The fallout of this revise creates the preconditions for scheming the parameters of thewaviness of manner feature. It resolve steady manner parameters such as clamor and shaking.

# REFERENCES


[1] Yue, Q., Li, L., Zhang, X. (2023). Failure mechanism and bearing capacity analysis of the underpinning structure with relative displacement. Engineering Failure Analysis, Vol. 148, 107205, https://doi.org/10.1016/j.engfailanal.2023.107205

[2] Gu, Q., Deng, Z., Lv, L., Liu, T., Teng, H., Wang, D., Yuan, J. (2021). Prediction research for surface topography of internal grinding based on mechanism and data model. International Journal of Advanced Manufacturing Technology, Vol. 113(3-4), pp. 821-836, https://doi.org/10.1007/s00170-021-06604-7

[3] Zhao, B., Wang, X., Ding, W., Wang, Y., Fu, Y., Zhao, Y., Zhu, J. (2023). Grain erosion wear properties and grinding performance of porous aggregated cubic boron nitride abrasive wheels. Chinese Journal of Aeronautics, https://doi.org/10.1016/j.cja.2022.08.005

[4] Wu, Z., Zhang, L. (2023). Analytical grinding force prediction with random abrasive grains of grinding wheels. International Journal of Mechanical Sciences, Vol. 250, 108310, https://doi.org/10.1016/j.ijmecsci.2023.108310

[5] Kishore, K., Sinha, M. K., Chauhan, S. R. (2023). A comprehensive investigation of surface morphology during grinding of Inconel 625 using conventional grinding wheels. Journal of Manufacturing Processes, Vol. 97, pp. 87-99 https://doi.org/10.1016/j.jmapro.2023.04.053

[6] Chalyj, V., Moroz, S., Ptachenchuk, V., Zablotskyj, V., Prystupa, S. (2020). Investigation of waveforms of roller bearing's working surfaces on hubfewer grinding operations. In: Ivanov V. et al. (eds) Advances in Design, Simulation and Manufacturing

III. DSMIE 2020. Lecture Notes in Mechanical Engineering, Springer, Cham, Vol. 1, pp. 349-360, https://doi.org/10.1007/978- 3-030-50794-7_34

[7] Kalchenko, V., Yeroshenko, A., Oyko, S. (2017). Mathematical modeling of abrasive grinding working process. Naukovyi Visnyk Natsionalnoho Hirnychoho Universytetu, Vol. 6, pp. 76-82.

[8] Zhang, X.-M., Zhang, Q.-J. (2010). Research on the simulation of hubfewer grinding process. Proceedings of the 29th Chinese Control Conference, Vol. 2010, pp. 5310-5313.

[9] Chunjian, H., Qiuju, Z., Yubing, X. (2010). Research on the computer simulation technique of cylindrical hubfewer grinding process. 2010 Second International Workshop on Education Technology and Computer Science, pp. 431-433, https://doi.org/10.1109/ETCS.2010.551

[10] Yang, H., Zhang, L., Li, D., Li, T. (2011). Modeling and analysis of grinding force in surface grinding. 2011 IEEE International Conference on Computer Science and Automation Engineering, pp. 175-178, https://doi.org/10.1109/CSAE.2011.5952448

[11] Zablotskyi, V., Tkachuk, A., Prozorovskyi, S., Tkachuk, V., Waszkowiak, M. (2022). Influence of turning operations on waviness characteristics of working surfaces of rolling bearings. In: Ivanov, V., Trojanowska, J., Pavlenko, I., Rauch, E., Peraković, D. (eds) Advances in Design, Simulation and Manufacturing V. DSMIE 2022. Lecture Notes in Mechanical Engineering. Springer, Cham, pp. 345-354, https://doi.org/10.1007/978-3-031-06025-0_34

[12] Shah, H., Taha, E. H. (2022). Busemann functions in asymptotically harmonic Finsler manifolds. Journal of Mathematical Physics, Analysis, Geometry, Vol. 18(4), pp. 546-561, https://doi.org/10.15407/mag18.04.546

[13] Zhuang, J., Cao, Y., Jia, M., Zhao, X., Peng, Q. (2023). Remaining useful life prediction of bearings using multi-source adversarial online regression under online unknown conditions. Expert Schemes with Applications, Vol. 227, 120276, https://doi.org/10.1016/j.eswa.2023.120276

[14] Gabor, M., Zdunek, R., Zimroz, R., Wodecki, J., Wylomanska, A. (2023). Non-negative tensor factorization for vibration-based local damage detection. Mechanical Schemes and Signal Processing, Vol. 198, https://doi.org/10.1016/j.ymssp.2023.110430

[15] Chen, J., Lin, C., Yao, B., Yang, L., Ge, H. (2023). Intelligent fault diagnosis of rolling bearings with low-quality data: A feature significance and diversity learning method. Reliability Engineering and Scheme Safety, Vol. 237, https://doi.org/10.1016/j.ress.2023.109343

[16] Bai, X., Zeng, S., Ma, Q., Feng, Z., An, Z. (2023). Intelligent fault diagnosis method for rolling bearing using WMNRS and LSSVM. Measurement Science and Technology, Vol. 34(7), https://doi.org/10.1088/1361-6501/acc3b9

[17] Zhu, D., Yin, B., Teng, C. (2023). An improved spectral amplitude modulation method for rolling element bearing fault diagnosis. Journal of the Brazilian Society of Mechanical Sciences and Engineering, Vol. 45(5), https://doi.org/10.1007/s40430- 023-04184-z

[18] Chen, S., Xie, B., Wang, Y., Wang, K., Zhai, W. (2023). Non-stationary harmonic summation: A novel method for rolling bearing fault diagnosis under variable speed conditions. Structural Health Monitoring, Vol. 22(3), pp. 1554-1580, https://doi.org/10.1177/14759217221110278

[19] Lin, S., Jiang, S. (2022). Rotordynamics of an improved face-grinding spindle: Rotational stiffness of thrust bearing increases radial stiffness of spindle. Journal of Manufacturing Science and Engineering, Transactions of the ASME, Vol. 144(8), https://doi.org/10.1115/1.4053458

[20] Zmarzły, P. (2022). Analysis of technological heredity in the production of rolling bearing rings made of AISI 52100 steel based on waviness measurements. Materials, Vol. 15(11), https://doi.org/10.3390/ma15113959

[21] Brosed, F. J., Zaera, V. A., Padilla, E., Cebrián, F., Aguilar, J. J. (2018). In-process measurement for the process control of the real-time manufacturing of tapered roller bearings. Materials, Vol. 11(8), https://doi.org/10.3390/ma11081371

**Citation:** Saravanan Suba, Dinesh Senduraja, V. Isakkirajan and P.Senthil Kumaran, Construction of Comportments Quantities Undulation Throughout Hub Rarer Mortise Crushing on Secure Manacles, International Journal of Information Technology (IJIT), 5(1), 2024, pp. 1-23

**Article Link:**
https://iaeme.com/MasterAdmin/Journal_uploads/IJIT/VOLUME_5_ISSUE_1/IJIT_05_01_001.pdf

**Abstract Link:**
https://iaeme.com/Home/article_id/IJIT_05_01_001



✉ editor@iaeme.com